growth of microorganisms is avoided by the addition of preservatives to the agarose solutions, for example 0.1% sodium azide or 0.01% sodium merthiolate.

Simple equipment is commercially available, though much can be made in-house. The electrophoresis system only requires two electrophoretic tanks (provided with platinum wire and connected to the electrodes), and an adjustable power supply delivering voltage up to 400 V at 400 mA. The connection between the agarose plates and the buffer in the tanks can be accomplished through filter-paper wicks previously wetted in electrophoretic buffer (the same as that used for preparing the gel). To avoid excessive warming of the gel during electrophoresis, it is convenient to cool the agarose plates using a system connected to tap water. This allows the electrophoresis to be run at room temperature in the laboratory, alternatively, it can be carried out in a cold room at 5°C.

A great number of polyvalent and specific antisera prepared in goat, sheep or rabbits can be obtained from different suppliers or obtained in-house.

Present and Future Developments

Though most immunoelectrophoretic techniques described here were developed at least 25 years ago, they still enjoy great popularity and continue to be excellent tools for biochemists and immunologists. IE and CIE are very useful techniques for the characterization of complex mixtures of proteins and for the study of certain pathological situations that evolve with changes in plasma protein patterns. CAIE is a powerful technique for detecting glycoprotein microforms using different lectin specificities. Advances in the characterization of new lectins with restricted specificity represent a future development in this field. CAIE can also be applied to many affinity systems, including the important contribution of monoclonal antibodies in the affinity electrophoresis step.

Immunoelectrophoretic techniques are time- and antisera-consuming techniques. These limitations could be improved by including the capillary methods commonly used in capillary electrophoresis systems.

Further Reading

Bøg-Hansen TC, Bjerrum OJ and Ramlau J (1975) Detection of biospecific interaction during the first dimension electrophoresis in crossed immunoelectrophoresis. *Scandinavian Journal of Immunology* 4 (Suppl. 2): 141.

Breborowicz J and Mackiewicz A (eds) (1992) *Affinity Electrophoresis: Principles and Application*. Boca Raton: CRC Press.

Dolník V (1997) Capillary zone electrophoresis of proteins. *Electrophoresis* 18: 2353.

Grabar P and Williams CA (1953) Méthode permettent l'étude conjugée des propiétés électrophoretiques et immunochimiques d'un mélange de protéines. Application au sérum sagnuin. *Biochimica Biophysica Acta* 10: 193.

Helenius A and Simons K (1977) Charge shift electrophoresis: simple method for distinguishing between amphiphilic and hydrophilic proteins in detergent solution. *Proceedings of the National Academy of Science of the USA* 74: 529.

Laurell CB (1966) Quantitative estimation of proteins by electrophoresis in agarose gel containing antibodies. *Analytical Biochemistry* 15: 45.

Ouchterlony Ö (1948) In vitro method for testing the toxin-producing capacity of diphtheria bacteria. *Acta Pathologica Microbiologica Scandinavica* 25: 186.

Ouchterlony Ö and Nilsson LÅ (1986) Immunodiffusion and immunoelectrophoresis. In: Weir M, Herzenerg LA, Blackwell C and Herzenberg LA (eds) *Handbook of Experimental Immunology* 4th edn, vol. 1. *Immunochemisty*, Ch. 32. Oxford: Blackwell Scientific Publications.

Ressler N (1960) Two-dimensional electrophoresis of proteins antigens with an antibody containing buffer. *Clinica Chimica Acta* 5: 795.

Uriel J (1971) Color reactions for identification of antigen–antibody precipitates in gels. In: Williams CA and Chase MW (eds) *Methods in Immunology and Immunochemistry*, vol. III, p. 294. New York: Academic Press.

Williams CA (1971) Immunoelectrophoretic analysis. In: Williams CA and Chase MW (eds) *Methods in Immunology and Immunochemistry*, vol. III, p. 235. New York: Academic Press.

Isoelectric Focusing

P. G. Righetti and A. Bossi, University of Verona, Verona, Italy
C. Gelfi, ITBA, CNR, Segrate, Milan, Italy

Isoelectric focusing represents a unique electrokinetic method in that it is based on steady-state patterns attained by amphoteric species (mostly proteins and peptides) along a pH gradient under the influence of an electric field. Due to a continuous balancing of diffusion away from the p*I* (isoelectric point) and p*I*-driven electric forces, extremely sharp zones are obtained, characterized by a very high resolving power. This article will consider conventional isoelectric focusing (IEF) in soluble, amphoteric buffers; and immobilized pH gradients (IPG) in insolubilized,

non-amphoteric buffers. In the latter case, guidelines will be given on how to optimize linear and nonlinear pH gradients and examples will be shown on the unique resolving power of the technique.

Conventional Isoelectric Focusing

In principle, pH gradients could be obtained by diffusion of non-amphoteric buffers but such 'artificial' gradients would be altered by changes in electric migration and diffusion of the buffer ions. Thus, Svensson in 1961 introduced the concept of 'natural' pH gradients, created and stabilized by the electric current itself. The buffers used in this system required two fundamental properties: first amphoterism, so that they could reach an equilibrium position along the separation column and secondly 'carrier' ability. This last concept is more subtle, but just as fundamental. Any ampholyte cannot simply be used for IEF; only a carrier ampholyte, that is a compound capable of transporting the current (a good conductor) and capable of carrying the pH (a good buffer). With this notion, and with Vesterberg's elegant synthesis of such ampholytes in 1969, present-day conventional IEF was born.

Some Basic Theoretical Concepts

Here some basic equations governing the IEF process will be considered. The most important is the one governing the distribution profile of an ampholyte about its isoelectric point. Under steady-state conditions (obtained by balancing the simultaneous electrophoretic and diffusional mass transports), Svensson derived the following differential equation describing the concentration profile of a focused zone:

$$C\mu i/qk = D\left(\frac{\mathrm{d}C}{\mathrm{d}x}\right) \qquad [1]$$

where C is the concentration of a component in arbitrary mass units per arbitrary volume unit; μ is the electric mobility in $\mathrm{cm^2\ V^{-1}\ s^{-1}}$ of ion constituent except H^+ and OH^-, with positive sign for cationic and negative sign for anionic migration; i is the electric current in A; q is the cross-sectional area in $\mathrm{cm^2}$ of electrolytic medium, measured perpendicularly to the direction of current; k is the conductance of the medium, in $\Omega^{-1}\ \mathrm{cm^{-1}}$; D is the diffusion coefficient in $\mathrm{cm^2\ s^{-1}}$ of a given ionic component with mobility μ; and x is the coordinate along the direction of current increasing from 0 to the anode towards the cathode.

Each term in eqn [1] expresses the mass flow per second and square centimetre of the cross-section: to the left being the electric and to the right the diffusional mass flows. If eqn [1] is re-written in the form:

$$\left(\frac{i\mu}{q}\right)\left(\frac{\mathrm{d}x}{k}\right) = D\left(\frac{\mathrm{d}C}{C}\right) \qquad [2]$$

it is seen that it is possible to integrate it if μ is known as a function of pH and D as a function of C. Specifically, if the conductance, the diffusion coefficient, and the derivative:

$$p = -\frac{\mathrm{d}\mu}{\mathrm{d}x} = -\left[\frac{\mathrm{d}\mu}{\mathrm{d(pH)}}\right]\left[\frac{\mathrm{d(pH)}}{\mathrm{d}x}\right] \qquad [3]$$

(where p is the ratio between the protein titration curve and the slope of the pH gradient over the separation axis) can be regarded as constant within the focused zone, then $\mu = -px$ and one obtains the following analytical solution:

$$C = C_0 \exp\left[-\frac{(pix^2)}{(2qkD)}\right] \qquad [4]$$

where x is now defined as being zero at the concentration maximum C_0. This is a Gaussian concentration distribution with inflection points at:

$$x_i = \pm\sqrt{\left(\frac{qkD}{pi}\right)} \qquad [5]$$

where x_i represents the width of the Gaussian distribution of the focused zone measured from the top of the distribution of the focused ampholyte to the inflection point (one standard deviation). The course of the pH gradient is $\mathrm{d(pH)}/\mathrm{d}x$ and $\mathrm{d}\mu/\mathrm{d(pH)}$ represents the titration curve of the ampholyte. It should be kept in mind that this Gaussian profile holds only if and as long as the conductivity of the bulk solution within the zone is constant. Constant conductivity along a pH gradient is quite difficult to maintain, especially as one approaches pH extremes (below pH 4 and above pH 10), if for no other reason, because the non-negligible concentration of H^+ and OH^- present in the bulk liquid begins to contribute strongly.

Another important equation regards the resolving power in IEF, expressed in $\Delta(\mathrm{p}I)$ units, i.e. in the minimum difference of surface charge between two adjacent proteins that the IEF technique is able to resolve. If two adjacent zones of equal mass have a peak-to-peak distance three times greater than the distance from the peak to inflection point there will be a concentration minimum approximating the two outer inflection points. Taking this criterion for resolved adjacent proteins, Rilbe derived the following equation for minimally but definitely resolved zones:

$$\Delta(\mathrm{p}I) = 3\sqrt{\left(\frac{D[\mathrm{d(pH)}/\mathrm{d}x]}{E[-\mathrm{d}\mu/\mathrm{d(pH)}]}\right)} \qquad [6]$$

This equation shows that good resolution should be obtained with substances with a low diffusion coefficient (D) and a high mobility slope [$d\mu/d(pH)$] at the isoelectric point – conditions that are satisfied by all proteins. Good resolution is also favoured by a high field strength (E) and a shallow pH gradient [$d(pH)/dx$]. It will be seen that, whereas in conventional IEF the limit to the resolving power is approximately 0.01, in IPGs it is 0.001 pH units.

The Carrier Ampholyte Buffers

Recall that the buffer capacity of an ampholyte in the isoprotic state decreases with increasing ΔpK across the isoprotic point, linearly at first, then exponentially. Let us take as an example a hypothetical ampholyte, with $pK_1 = 4.6$ (a carboxyl group) and $pK_2 = 6.2$ (an amino group), having thus a $pI = 5.4$ and $\Delta pK = 1.6$. If we titrate this ampholyte in the pH 4–7 range, encompassing the two pKs, and if we plot the accompanying buffering power (β), degree of dissociation (α) and slope of the pH gradient, we will have the plot shown in **Figure 1**(A). It can be seen that there is still a substantial buffering power at the pI of the ampholyte, with a corresponding degree of ionization less than unity, and that the titration curve is smooth throughout the pH gradient explored, with only a small deviation about the pI of the ampholyte, indicating that this species is indeed a 'good' carrier ampholyte. Now take an ampholyte with $pK_1 = 4.6$ but with $pK_2 = 9.3$, thus with a $pI = 6.95$ and $\Delta pK = 4.7$. If we now titrate it in the pH 4–10 range, again encompassing the two pK values, we will have the graph shown in **Figure 1**(B). It can be seen now that at the theoretical pI value the ampholyte does not have any appreciable buffering power and that it is fully ionized. In addition, it is not only isoelectric at pH = 6.95, but indeed almost at any pH in the interval 5–9, as seen by the abrupt sigmoidal shape in the pI environment. This species will be a 'bad' carrier ampholyte, useless for a well-behaved IEF fractionation.

An important prerequisite for a good carrier ampholyte is that it has a high conductivity at its pI. Regions of low conductivity will absorb much of the applied voltage, thus reducing the field strength and hence the potential resolution in other parts of the gradient. It has been demonstrated that good conductivity is associated with small values of pI–pK. This is also true for the buffering capacity of an ampholyte. Thus, the parameter pI–pK (equivalent to $\frac{1}{2}\Delta pK$) becomes the most important factor in selecting carrier ampholytes exhibiting both good conductivity and buffering capacity (β).

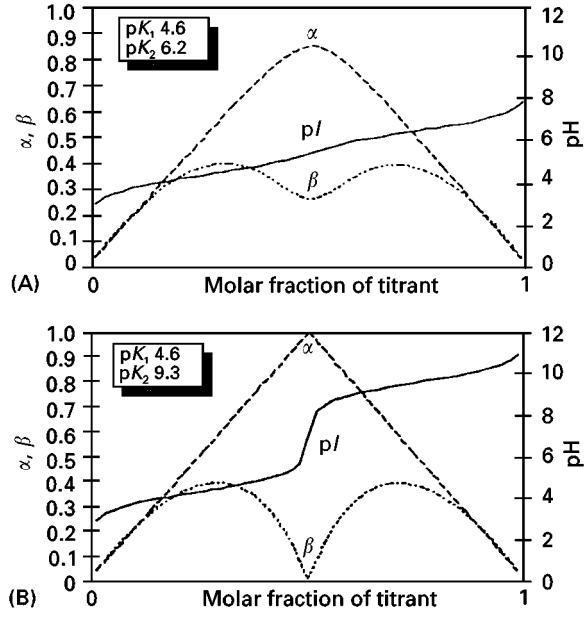

Figure 1 Degree of ionization (α) and buffering power (β) of a good (A) and a poor (B) carrier ampholyte. (A) computer simulations obtained assuming a $pK_1 = 4.6$ and a $pK_2 = 6.2$ ($pI = 5.4$). The ampholyte was titrated in the pH 4–7 interval. (B) Computer simulation obtained by assuming a $pK_1 = 4.6$ and a $pK_2 = 9.3$ ($pI = 6.95$). The ampholyte was titrated in the pH 4–10 interval. Note the sharp sigmoidal transition in the pI region in (B), suggesting total lack of buffering power (Wenger P and Righetti PG, unpublished observations).

Methodology

The structure of carrier ampholytes (CA) and their general properties are illustrated in **Figure 2**. CAs are oligoprotic amino carboxylic acids, each containing at least four weak protolytic groups, at least one being a carboxyl group and at least one a basic nitrogen atom, but no peptide bonds. In a typical synthesis, a mixture of oligoamines (four to six nitrogens in length, linear and branched) reacts with an α–β-unsaturated acid (typically acrylic or itaconic acids), at a nitrogen–carboxyl ratio of 2 : 1.

The mechanism of developing a pH gradient in IEF is illustrated in **Figure 3**. Before passage of the current, the column is at constant pH (**Figure 3**A) and the multitude of amphoteric buffers is randomly distributed, resulting in a reciprocal neutralization. However, each individual CA species will have its own titration curve (see **Figure 2**, lower left side) defining different mobilities in the electric circuit. After starting the experiment the different CAs will migrate at different velocities in the column, the most acidic and most basic compounds being the fastest moving ions. As a result of this sorting process, a pH gradient will form, sigmoidal at first (**Figure 3**B), with an uneven voltage gradient. After 1 h, the various CA buffers will have separated further, and at this point an almost linear pH gradient has been established

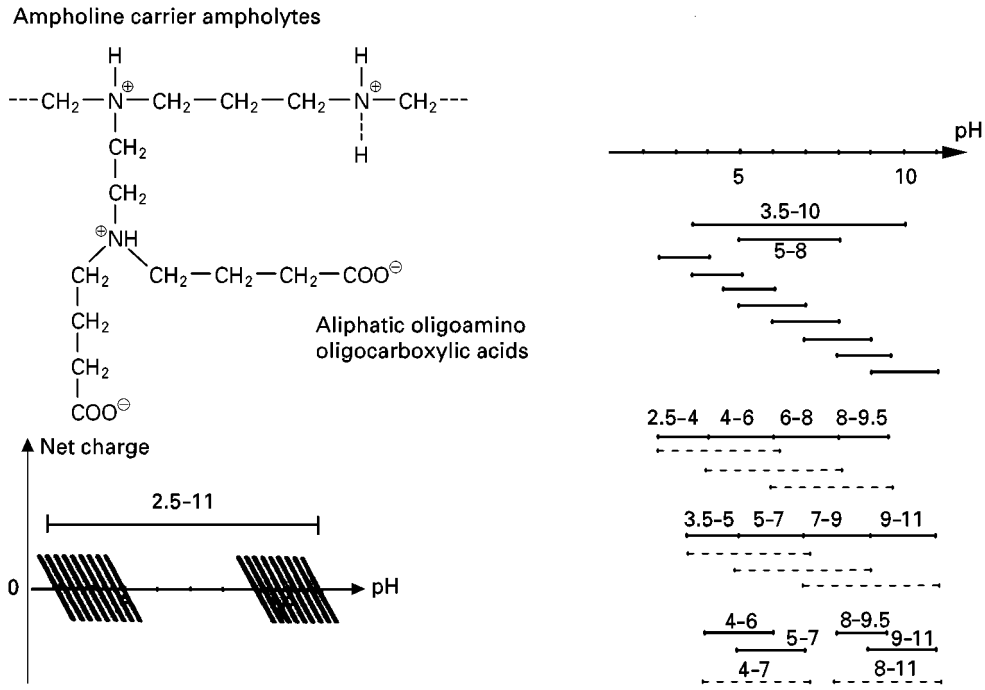

Figure 2 Composition of Ampholine. On the upper left side a representative chemical formula is shown (aliphatic oligoamino oligocarboxylic acids). On the lower left side, portions of hypothetical titration curves of carrier ampholytes are depicted. Right: different pH cuts for wide and narrow range ampholytes (by permission of LKB Produkter AB).

which spans the pH range defined by the p*I*s of the ampholytes (**Figure 3**C). After 1.5 h the CAs have separated into symmetrical zones with overlapping Gaussian profiles. Now the system has achieved a steady-state, i.e. a balance between electrophoretic transport and diffusion away from the p*I*, and no

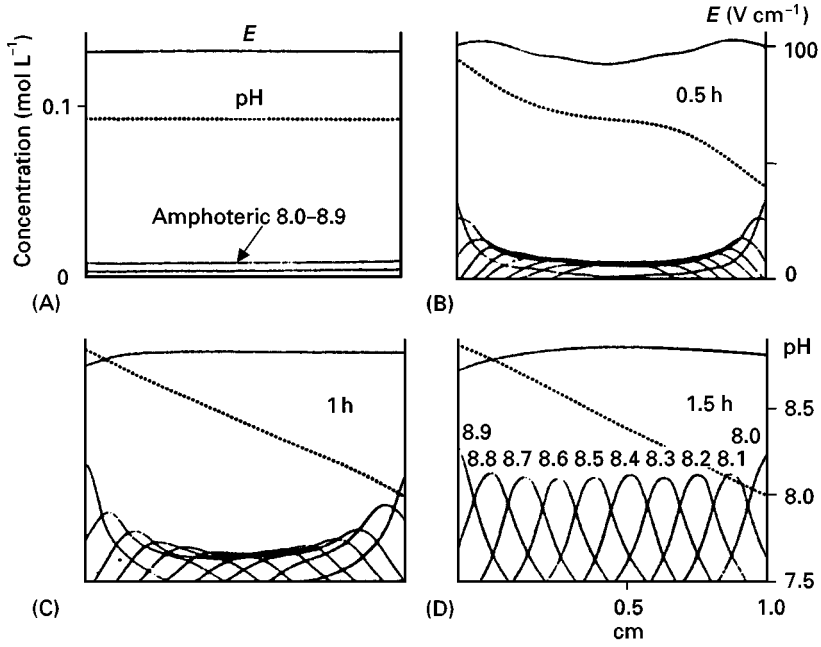

Figure 3 Calculated time development of a focusing process involving 10 ampholytes in a closed vessel. The p*I*s of the ampholytes are evenly distributed in the pH 8.0–8.9 range. The initial distribution of the amphoteric buffers is indicated in (A). The calculation was performed assuming a constant voltage (100 V cm^{-1}) across the system. The anode is positioned to the right in the diagrams. Each *x*-axis represents the distance from the cathode on the same scale as in (D). (Reproduced with permission from Schaefer-Nielsen, 1986.)

further mass transport is expected (**Figure 3**D). As long as the local concentration of the different CA species does not change the slope of the pH gradient will be kept constant with time. Proteins will keep migrating against this CA distribution profile eventually reaching their p*I* position.

By and large, most analytical IEF runs are performed in horizontal chambers: the polyacrylamide gel slab rests on a cooling block [generally made of glass or coated aluminium or even beryllium oxide (used as the heat shield of the space shuttle)]. This horizontal configuration allows one to dispose of electrode reservoirs and of all the hydraulic problems connected with vertical chambers (tight seals, etc.): in fact, anolyte and catholyte are soaked in filter paper strips resting directly on the open gel surface. In addition, most modern chambers contain a cover lid with movable electrodes which can be adjusted to any gel length (generally from 10 to 25 cm electrode distance). Since thick gels (e.g. 2 mm thick) generate thermal gradients through the gel thickness, resulting in skewed zones (essentially all horizontal chambers have cooling only on one gel face) ultrathin gels (0.2–0.5 mm) supported on a reactive polyester foil (Gel Bond PAG) are preferred today.

Immobilized pH Gradients (IPG)

IPGs are based on the principle that the pH gradient, which exists prior to the IEF run itself, is copolymerized, and thus immobilized within the polyacrylamide matrix. This is achieved by using as buffers a set of up to 10 non-amphoteric, weak acids and bases, called Immobilines, having the following general chemical composition: CH_2=CH–CO–NH–R, where R denotes either three different weak carboxyls, with p*K*s of 3.1, 3.6, and 4.6 (**Table 1**), or five tertiary amino groups, with p*K*s of 6.2, 7.0, 8.5, 9.3 and 10.3 (**Table 2**). This set of eight weak buffers is complemented by a strong acid (p*K* of approximately 1, 2-acrylamido-2-methyl propanesulfonic acid) and a strong base (p$K > 12$, quaternary aminoethylacrylamide), used only as titrants. During gel polymerization, these buffering species are incorporated into the gel (84–86% conversion efficiency at 50°C for 1 h), by the same free radical reaction used to activate the acrylamide double bond. **Figure 4** shows a segment of a hypothetical structure of an Immobiline matrix and the process of focusing two proteins in it. It is seen that only the proteins migrate to their steady-state position, whereas the Immobilines remain fixed at their original grafting position in the gel, where a fixed ratio of buffering/titrant ions defines the pH locally. This means that the pH gradient is stable indefinitely (but it has to pre-exist before the onset of polymerization) and can only be destroyed if and when the polyacrylamide gel is hydrolyzed. Given the sparse distribution of Immobilines in the gel they behave as isolated charges, able to effectively contribute to the ionic strength of the medium. In conventional IEF, on the contrary, at steady-state the ionic strength is exceedingly low (less than 1 mequiv L^{-1}) since the focused carrier ampholytes form an inner salt, and this often results in protein precipitation and smears both at the p*I* and in its proximity. In IPGs the high ionic strength existing in the matrix (typically 10 mequiv L^{-1}) induces protein solubilization at the p*I* value (thus CA-IEF is similar to a 'salting-out' milieu and IPGs to a 'salting-in' environment).

Immobiline-based pH gradients can be cast in the same way as conventional polyacrylamide gradient gels by using a density gradient to stabilize the Immobiline concentration gradient, with the aid of a standard, two-vessel gradient mixer. As shown earlier, these buffers are no longer amphoteric as in

Table 1 Acidic acrylamido buffers

pK	*Formula*	*Name*	M_r
1.0	$CH_2{=}CH{-}CO{-}NH{-}C(CH_3)(CH_2{-}SO_3H){-}CH_3$	2-Acrylamido–2-methylpropanesulfonic acid	207
3.1	$CH_2{=}CH{-}CO{-}NH{-}CH(OH){-}COOH$	2-Acrylamidoglycolic acid	145
3.6	$CH_2{=}CH{-}CO{-}NH{-}CH_2{-}COOH$	*N*-Acryloylglycine	129
4.6	$CH_2{=}CH{-}CO{-}NH{-}(CH_2)_3{-}COOH$	4-Acrylamidobutyric acid	157

Table 2 Basic acrylamido buffers

pK	*Formula*	*Name*	M_r
6.2	$CH_2{=}CH{-}CO{-}NH{-}(CH_2)_2{-}N\langle\ \rangle O$	2-Morpholinoethylacrylamide	184
7.0	$CH_2{=}CH{-}CO{-}NH{-}(CH_2)_3{-}N\langle\ \rangle O$	3-Morpholinopropylacrylamide	198
8.5	$CH_2{=}CH{-}CO{-}NH{-}(CH_2)_2{-}N(CH_3)_2$	*N,N*-Dimethylaminoethylacrylamide	142
9.3	$CH_2{=}CH{-}CO{-}NH{-}(CH_2)_3{-}N(CH_3)_2$	*N,N*-Dimethylaminopropylacrylamide	156
10.3	$CH_2{=}CH{-}CO{-}NH{-}(CH_2)_3{-}N(CH_2H_5)_2$	*N,N*-Diethylaminopropylacrylamide	184
> 12	$CH_2{=}CH{-}CO{-}NH{-}(CH_2)_2{-}\overset{+}{N}(CH_2H_5)_3$	*N,N-N*-Triethylaminoethylacrylamide	198

conventional IEF, but are bifunctional: the buffering group is located at one end of the molecule and at the other end there is the acrylic double bond which will disappear during the grafting process. The three carboxyl immobilines have rather small temperature coefficients of ionization (dpK/dT) in the 10–25°C range due to their small standard heats of ionization (approximately 1 kcal mol^{-1}) and thus exhibit negligible p*K* variations over this temperature range. On the other hand, the four basic immobilines exhibit rather large ΔpKs in the same temperature range (as much as $\Delta pK = 0.44$ for the p*K* 8.5 species) due to their larger heats of ionization (6–12 kcal mol^{-1}). Therefore, for reproducible runs and pH gradient calculations, all the experimental parameters have been fixed at 10°C. Temperature is not the only variable that will affect immobiline p*K*s (and therefore the actual pH gradient generated): additives in the gel that will change the water structure (chaotropic agents such as urea) or lower its dielectric constant, and the ionic strength itself of the solution, will alter p*K* values.

Narrow and Ultranarrow pH Gradients

We define the gradients (in the gel slab) from 0.1 to 1 pH unit as ultranarrow and narrow gradients, respectively. Within these limits one can generally work on a 'tandem' principle, i.e. choosing a 'buffering' Immobiline (e.g. a base or an acid), having its p*K* within the desired pH interval, and a 'non-buffering' Immobiline (e.g. an acid or a base), having its p*K* at least 2 pH units removed from either pH_{min} or pH_{max} of the pH range. The latter will therefore provide equivalents of acid or base, respectively, to titrate the buffering group, but will not itself buffer in the desired pH interval. For these calculations one

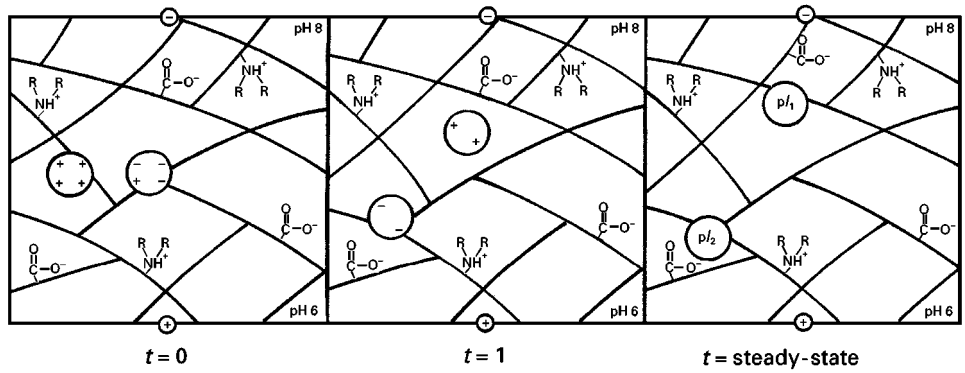

Figure 4 Hypothetical structure of an Immobiline gel and mechanism of the focusing process. The acrylamido acid and basic groups are shown grafted on the polyacrylamide matrix. Two proteins are shown migrating in the gel at the times $t = 0$, at $t = 1$ and finally at the steady-state, where they reach they respective p*I* values (pI_1 and pI_2) as points of zero net charge (by permission of LKB Produkter AB).

can resort to modified Henderson–Hasselbalch equations and to rather complex nomograms or simply adopt tabulated recipes, 1 pH unit wide, which start with the pH 3.8–4.8 interval and end with the pH 9.5–10.5 span, separated by 0.1 pH unit increments (58 such recipes have been tabulated). If a narrower pH gradient is needed this can be derived from any of the 58 pH intervals tabulated by a simple linear interpolation of intermediate Immobiline molarities.

Extended pH Gradients

For wider pH intervals, several buffering species have to be mixed and the situation becomes considerably more complex. This has been solved with the aid of computer programs designed specifically for this purpose. The basic findings are: first for generating a linear pH gradient the buffering power has to be constant throughout the desired pH interval (this is best achieved when the pK values are spaced at 1 pH unit intervals, see **Figure 5**). Secondly, to avoid deviations from linearity, the titrants should have pKs well outside pH_{min} and pH_{max} of the wanted pH range (in general, at least 2 pH units removed from the limits of the pH interval) (see **Figure 6**). As a consequence of this, for pH ranges wider that 3 pH units, two additional Immobilines are needed as titrants: one strongly acidic ($pK < 1$) and one strongly basic ($pK > 12$). There are two ways of generating extended pH intervals. In one approach the concentration of each buffer is kept constant throughout the span of the pH gradient and 'holes' of buffering power are filled by increasing the amounts of the buffering species bordering the largest ΔpKs; in the

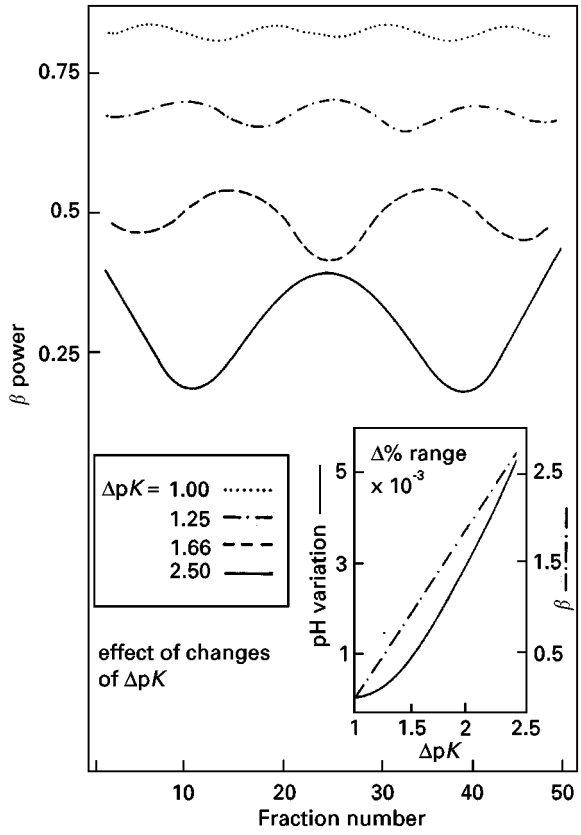

Figure 5 Effect of changes in the number of (evenly spaced) buffering components. The optimal concentrations of fictitious buffers (bases) with pKs differing by 1, 1.25, 1.66 and 2.5 pH units, were calculated so as to cover the pH 4.5–8.5 range. The resulting courses of β power are shown as a function of ΔpK. The insert is a plot of percentage variation, in comparison with the case $\Delta pK = 1$, of the ranges of deviation of pH (left scale) and of β (right scale). Note that the smoothest β power is obtained with $\Delta pK = 1$ (from Gianazza *et al.*, 1983, with permission of Elsevier Science Publishers).

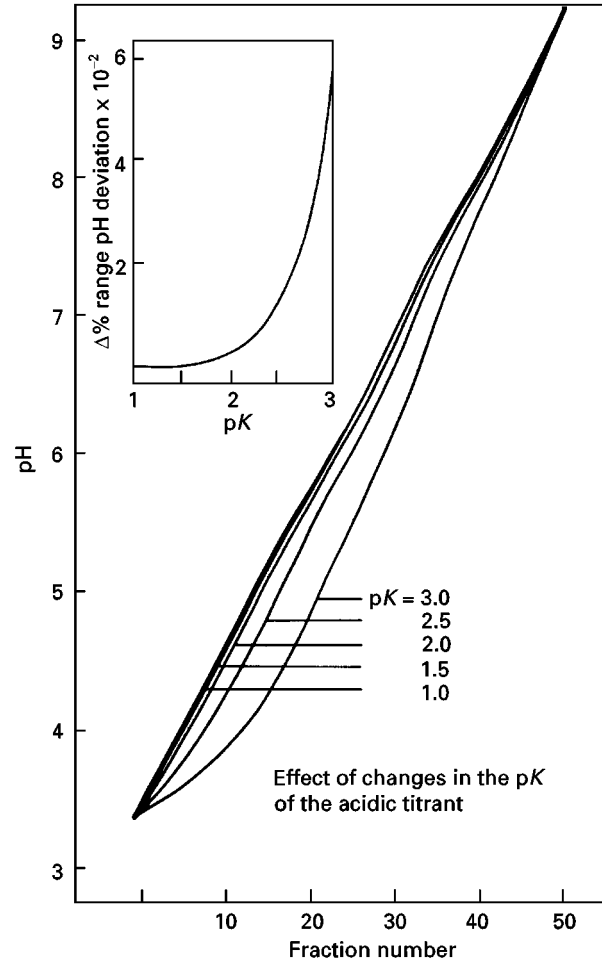

Figure 6 Effect of changes in the pK of the acidic titrant. A reference Immobiline mixture was titrated to the same pH value with fictitious acids whose pK was 0.5, 1.0, 1.5, 2.0 and 2.5 pH unit lower than the gradient's limit (in this case, $pH_{min} = 3.5$) and the pH course was calculated for the five cases. The insert is a plot of the percentage variation of deviation from linearity as the titrant's pK increases (from Gianazza *et al.*, 1983, with permission of Elsevier Science Publishers).

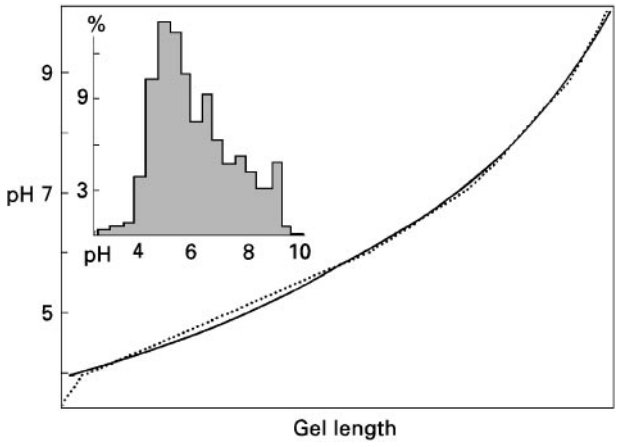

Figure 7 Non-linear pH 4–10 gradient. Ideal (dotted line) and actual (solid line) formulation courses. The shape for the ideal profile was computed from data on the statistical distribution of proteins p*I*s. The relevant histogram is redrawn in the figure inset (from Gianazza *et al.*, 1985; by permission of VCH).

other approach (varying buffer concentration) the variation in concentration of the various buffers along the width of the desired pH gradient results in a shift of their apparent p*K*s with a concomitant evening-out of the ΔpK values. With the available recipes, preparation of any Immobiline gel is now a trouble-free operation, as all the complex computing routines have already been performed and no further calculations of any type are required.

Non-linear, Extended pH Gradients

IPG formulations have been given only in terms of rigorously linear pH gradients. While this has been the only solution adopted so far, it might not be the optimal one in some cases. Altering the pH slope in some portions of the gradient might be required in those pH regions overcrowded with proteins. The reasons for resorting to non-linear pH gradients are given in the histogram of **Figure 7**. With the relative abundance of different species it is clear that an optimally resolving pH gradient should have a gentler slope in the acidic portion, and a steeper course in the alkaline region. Such a general course has been calculated by assigning to each 0.5 pH unit interval in the pH 3.5–10 region a slope inversely proportional to the relative abundance of proteins in that interval. The ideal (dotted) curve in **Figure 7** was obtained by such a procedure. What is also important here is the establishment of a new principle in IPG technology, namely that the pH and density gradients stabilizing it need not be co-linear. The possibility exists of modulating the former by locally flattening of pH

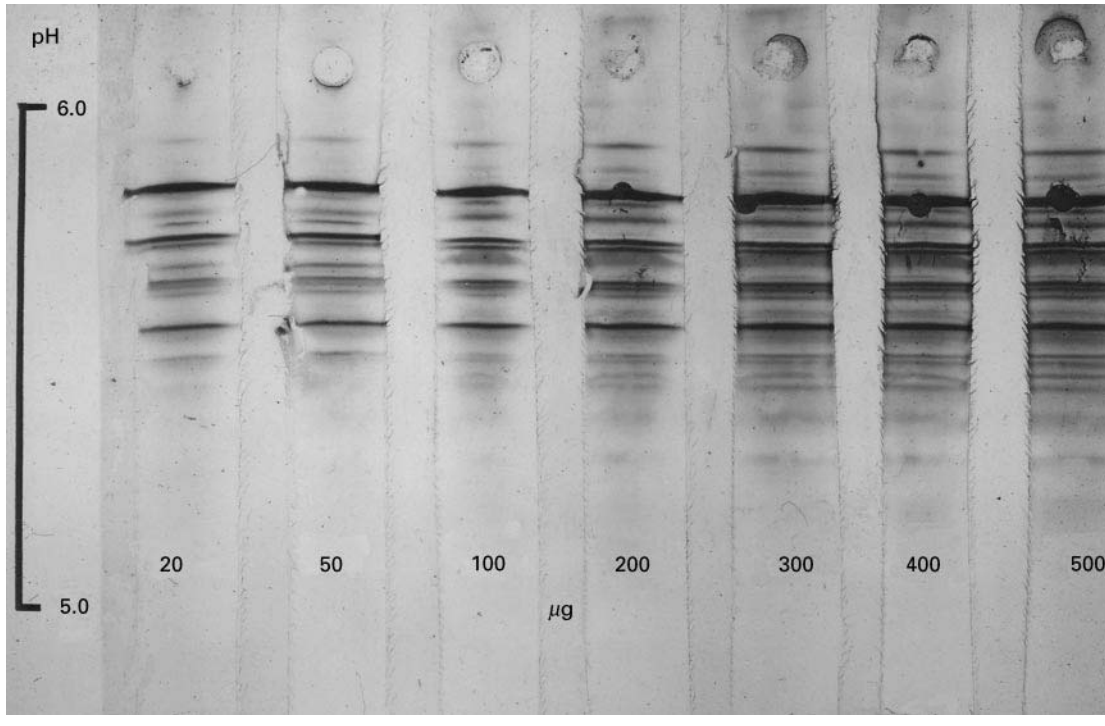

Figure 8 IEF of conalbumin in an IPG pH 4.5–6.5 gradient. Gel: 5%T, 3%C polyacrylamide, equilibrated in 10% glycerol. All samples were applied in round basins punched through the gel thickness at the cathodic side as 20 μL droplet (20–500 μg protein). Staining with Coomassie Blue R-250 in ethanol/acetic acid in presence of copper sulfate. Notice that, although the gel thickness is only 0.5 mm, there is no overloading effect in such a wide interval of protein concentration (from Righetti PG and Ek K, unpublished observations).

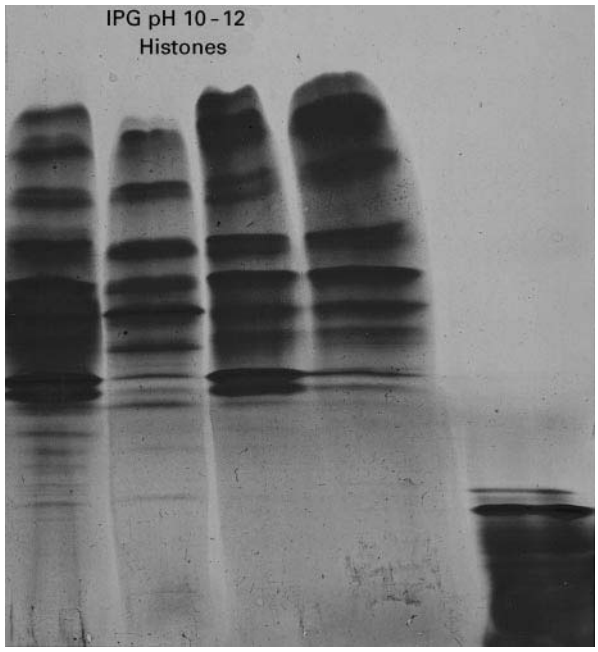

Figure 9 Focusing of histones in an IPG pH 10–12 nonlinear interval. Gel: 6% T, 4% C polyacrylamide matrix, containing an IPG 10–12 gradient, reswollen in 7 M urea, 1.5% Nonidet P-40 and 0.5% Ampholine pH 9–11. The gel was run at 10°C under a layer of light paraffin oil at 500 V for the first hour, followed by increasing voltage gradients, after sample penetration, up to 1300 V for a total of 4 h. The samples (2 mg mL^{-1}, 50 μL seeded) were loaded in plastic well at the anodic gel surface. Staining with Coomassie Brilliant Blue R-250 in Cu^{2+}. Histone samples (from left). (1) VII-S (Lys-rich); (2) VI-S; (3) II-AS and (4) VIII-S (Arg-rich, subgroup F), from calf thymus. The p*I* 10.6 marker (cytochrome C) is in track 5 on the right side (from Bossi *et al.*, 1994, by permission of Elsevier Science Publishers).

gradients for increased resolution, while leaving unaltered the latter.

Although only one example of a nonlinear extended pH gradient is given here, clearly the possibility exists of modulating in the same fashion any narrower pH interval.

Examples on the Resolving Power

What can IPGs achieve in practice? **Figure 8** gives an example of a separation carried to the limit of a small-scale preparative load. Even when conalbumin is greatly overloaded, up to 500 μg in a single track, no smears or precipitations occur, while faint bands become visible. Another interesting example, at the very limit of any focusing technique, is given in **Figure 9**. Here histones are seen focused at the steady-state in a very alkaline pH 10–12 gradient. It can be appreciated that all histones have a p*I* in the pH range 11–12, as they should, given their amino acid composition. Previous data obtained by conventional IEF had attributed to them p*I*s in the pH 9–10 interval, clearly grossly underestimated.

Further Reading

Bossi A, Gelfi C, Orsi A and Righetti PG (1994) Isoelectric focusing of histones in extremely alkaline immobilized pH gradients: comparison with capillary electrophoresis. *Journal of Chromatography A* 686: 121–128.

Gianazza E, Dossi G, Celentano F and Righetti PG (1983) Isoelectric focusing in immobilized pH gradients: generation and optimization of wide pH intervals with two-chamber mixers. *Journal of Biochemical Biophysical Methods* 8: 109–133.

Gianazza E, Giacon P, Sahlin B and Righetti PG (1985) Non-linear pH courses with immobilized pH gradients. *Electrophoresis* 6: 53–56.

Righetti PG (1983) *Isoelectric Focusing*: *Theory*, *Methodology and Applications*. Amsterdam: Elsevier.

Righetti PG (1990) *Immobilized pH Gradients*: *Theory and Methodology*. Amsterdam: Elsevier.

Righetti PG, van Oss CJ and Vanderhoff JW (eds) (1979) *Electrokinetic Separation Methods*. Amsterdam Elsevier.

Rilbe H (1976) Theory of isoelectric focusing. In: Catsimpoolas N (ed.) *Isoelectric Focusing*, pp. 14–52. New York: Academic Press.

Rilbe H (1996) *pH and Buffer Theory*: *a New Approach*. Chichester: John Wiley.

Schaefer-Nielsen C (1986) Computer simulation of pH gradient formation in isoelectric focusing. In: Dunn MJ (ed.) *Gel Electrophoresis of Proteins*, pp. 1–36. Bristol: Wright.

Svensson H (1961) Isoelectric fractionation, analysis and characterization of ampholytes in natural pH gradients. Scandinavica I. The differential equation of solute concentration at steady state and its solution for simple cases. *Acta Chemica Scandinavica* 15: 325–341.

Vesterberg O (1969) Synthesis of carrier ampholytes for isoelectric focusing. *Acta Chemica Scandinavica* 23: 2653–2666.

Isoelectric Focusing in Capillary Electrophoresis

See **II / ELECTROPHORESIS / Capillary Isoelectric Focusing**